Acta Astronautica 82 (2013) 173–182

Contents lists available at SciVerse ScienceDirect

Acta Astronautica

journal homepage: www.elsevier.com/locate/actaastro

Z-Pinch fusion-based nuclear propulsion

J. Miernik [a,*], G. Statham [a], L. Fabisinski [b], C.D. Maples [c], R. Adams [d], T. Polsgrove [d], S. Fincher [d], J. Cassibry [e], R. Cortez [e], M. Turner [e], T. Percy [f]

[a] ERC Inc., USA
[b] ISS Inc., USA
[c] Qualis Corp Jacobs ESTS Group, USA
[d] NASA MSFC, USA
[e] Propulsion Research Center, University of Alabama Huntsville, USA
[f] SAIC, USA

ARTICLE INFO

Article history:
Received 25 December 2011
Accepted 12 February 2012
Available online 28 March 2012

Keywords:
Z-pinch
Magneto-inertial
Fusion
Propulsion

ABSTRACT

Fusion-based nuclear propulsion has the potential to enable fast interplanetary transportation. Due to the great distances between the planets of our solar system and the harmful radiation environment of interplanetary space, high specific impulse (I_{sp}) propulsion in vehicles with high payload mass fractions must be developed to provide practical and safe vehicles for human space flight missions.

The Z-Pinch dense plasma focus method is a Magneto-Inertial Fusion (MIF) approach that may potentially lead to a small, low cost fusion reactor/engine assembly [1]. Recent advancements in experimental and theoretical understanding of this concept suggest favorable scaling of fusion power output yield [2]. The magnetic field resulting from the large current compresses the plasma to fusion conditions, and this process can be pulsed over short timescales (10^{-6} s). This type of plasma formation is widely used in the field of Nuclear Weapons Effects testing in the defense industry, as well as in fusion energy research. A Z-Pinch propulsion concept was designed for a vehicle based on a previous fusion vehicle study called "Human Outer Planet Exploration" (HOPE), which used Magnetized Target Fusion (MTF) [3] propulsion. The reference mission is the transport of crew and cargo to Mars and back, with a reusable vehicle.

The analysis of the Z-Pinch MIF propulsion system concludes that a 40-fold increase of I_{sp} over chemical propulsion is predicted. An I_{sp} of 19,436 s and thrust of 3812 N s/pulse, along with nearly doubling the predicted payload mass fraction, warrants further development of enabling technologies.

1. Introduction

Selected results of a study conducted in 2010 [4] by members of the Advanced Concepts Office (ACO) at MSFC are presented describing the conceptual design of a Z-Pinch Magneto-Inertial Fusion (MIF) propulsion system. Fig. 1 depicts a vehicle including all necessary systems for an integrated interplanetary spacecraft for human exploration. The basic design and mass of an earlier interplanetary vehicle conceived in a study called HOPE was used to develop the main propulsion engine utilizing the Z-Pinch MIF concept. This NASA study also offered recommendations for a Z-Pinch pulsed plasma propulsion technology development program that could be conducted at RSA utilizing a DM2 test article.

Z-Pinch physics and earlier fusion studies [5–7] were considered in the development of a simplified Z-Pinch

* Correspondence to: Marshall Space Flight Center, Advanced Concepts Office, ED04, Huntsville, AL 35812, USA. Tel.: +1 11 256 544 6534; fax: +1 11 256 961 2266.
E-mail address: janie.h.miernik@nasa.gov (J. Miernik).

0094-5765/$ - see front matter © 2012 Elsevier Ltd. All rights reserved.
doi:10.1016/j.actaastro.2012.02.012

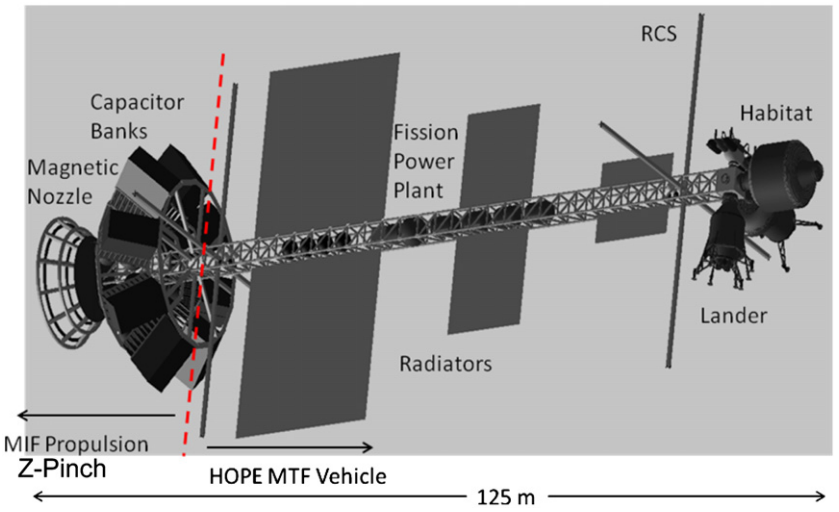

Fig. 1. Z-Pinch vehicle configuration.

fusion thermodynamic model to determine the quantity of plasma, plasma temperature, rate of expansion, and energy production to calculate parameters and characterize a propulsion system. The amount of nuclear fuel per pulse, mixture ratio of the Deuterium–Tritium (D–T) and Lithium-6/7 (Li^6) propellant, and assumptions about the efficiency of the engine facilitated the sizing of the propulsion system and resulted in an estimate of thrust and I_{sp} for the MIF Z-Pinch fusion propulsion engine of an interplanetary vehicle.

A magnetic nozzle is essential for fusion engines to contain and direct the nuclear by-products created in pulsed fusion propulsion. The nozzle must be robust to withstand the extreme stress, heat, and radiation. The configuration of fuel injection directs the D–T and Li^6 within the magnetic nozzle to create the Z-pinch reaction as well as complete an electrical circuit to allow some of the energy of the nuclear pulses to rapidly recharge the capacitors for the next power pulse. Li^6 also serves as a neutron shield with the reaction between neutrons and Li^6 producing additional Tritium and energy, adding fuel to the fusion reaction and boosting the energy output.

Trajectory analysis with the propulsion model was used to determine the duration of the propulsion burns, the amount of propellant expended, and the mixture ratio of the D–T and liner fuel to accomplish a particular mission. A number of missions, modeling variables, vehicle configurations, and design parameters were traded during the previously mentioned NASA studies; however, this paper concentrates on the conceptual Z-Pinch MIF nuclear engine of the proposed vehicle. An outline of the mission and vehicle configuration is offered to provide a framework for the propulsion design.

2. Theory/calculation

The approach investigated in this study involves the use of a confinement scheme known as a Z-Pinch, which falls under the MIF regime. The Z-Pinch's basic function is to manage and run very large currents (Megampere scale) through plasma over short timescales (10^{-6} s). The magnetic field resulting from the large current then compresses the plasma to fusion conditions. For a fusion propulsion system, the Z-Pinch is formed using an annular nozzle with D–T fuel injected through the innermost nozzle and Li^6 introduced through a cylindrical outer nozzle like a "shower curtain." The Li^6 propellant injection is focused in a conical manner, so that the D–T fuel and Li^6 mixture meet at a specific point that acts as a cathode. Li^6 will serve as a current return path to complete the circuit, as shown in two different graphical representations in Figs. 2 and 3.

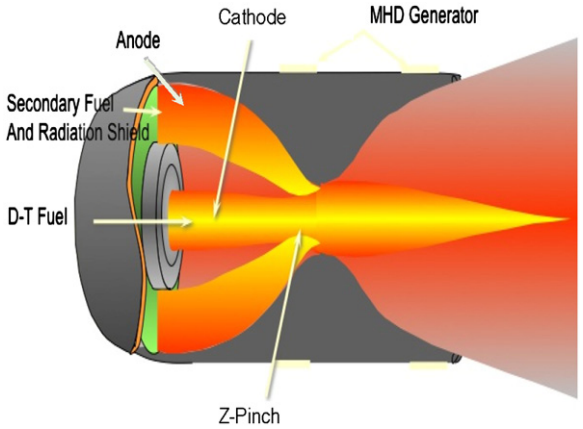

Fig. 2. Z-Pinch cathode runs axially down center.

The Li^6 propellant becomes a nozzle "liner" and serves as a neutron "getter," as well as the current return path. The advantage of this configuration is the reaction of Li^6 and high energy neutrons produces additional Tritium fuel and energetic by-products that boost the energy output. Through careful introduction and mixture ratio of the injected D–T fuel and Li^6 propellant, the Z-Pinch reaction via MIF fusion can produce very high specific impulse by means of rapid exit velocity.

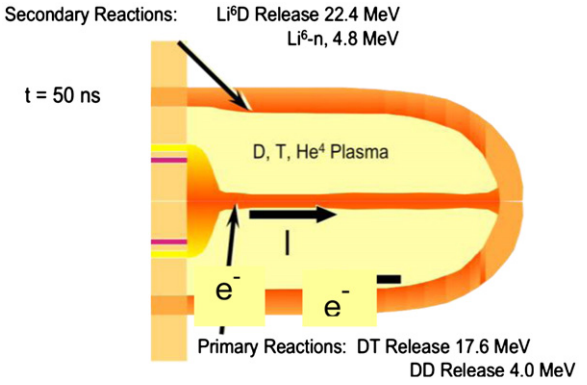

Fig. 3. Li^6 liner provides anode return path.

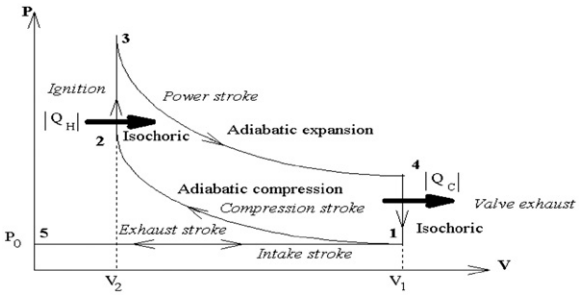

Fig. 4. Otto Cycle.

Analysis of fusion plasmas and their dynamic Magneto-Hydrodynamic (MHD) flows, as well as the fusion reactions themselves, necessitate the formulation of simple models and approximations to facilitate understanding. An approximation is made to develop a qualitative understanding of multiple fusion ignition processes. This is similar to the air-standard analysis of an internal-combustion engine, also known as the Otto cycle, shown in Fig. 4.

A similar approximation may be made to develop a qualitative understanding of multiple fusion ignition processes. Thus, within the framework of thermodynamics, it is possible to develop a straightforward engineering cycle analysis as was developed for the internal-combustion engine. Using the ideal thermodynamic model that describes the Otto cycle, the performance of a Z-pinch fusion reaction engine is described. The implications, assumptions, inputs, and results used for this study determine the design points of the study.

Per the Otto cycle and energy balance for each step:

- Process 1–2: isentropic compression $[1-2]: w_{12}=u_2-u_1$
- Process 2–3: constant volume heat addition $[2-3]: q_{23}=u_3-u_2$
- Process 3–4: isentropic expansion $[3-4]: w_{34}=u_3-u_4$
- Process 4–1: constant volume heat rejection $[4-1]: q_{41}=u_4-u_1$

For process [1–2], knowing the ignition temperature required, a value for the initial temperature of the plasma can be estimated.

$$T_1 = T_2 r^{-2(\gamma-1)}.$$

Treating the plasma at state 1 as an ideal gas, so that $p_1=\rho_r R T_1$, and using the pressure balance stated above, estimate values of magnetic field at state 1, current required to generate the field, and the magnetic field energy:

$$B_1 = \sqrt{2\mu_0 p_1}$$

$$I_1 = \frac{B_1}{\mu_0}(2\pi R_1)$$

$$E_{mag,1} = \frac{B_1^2}{2\mu_0}(\pi R_1^2 l)$$

Following the same procedure enables the estimation of these values at state 2.

For process [2–3], constant volume heat addition, we can evaluate the following relation only by knowing the temperature at states 2 and 3.

$$q_{23} = c_v(T_3 - T_2)$$

Although the temperature is known in state 2, fixing a temperature at state 3 after expansion of the reacting plasma, would be superfluous due to the ambiguity of the properties of the plasma after the explosion. Also, a real fusion reaction engine would not be a closed system. However, rather than choosing an arbitrary temperature to fix the end state of the process, the temperature can be calculated by knowing the nature of the fusion reactions. In Table 1 the primary reactions considered are listed. Although the lithium liner mass is expected to participate in many energetic secondary reactions, we are assuming that this material acts as an inert observer in the process, not reacting with the D–T fuel. In this way the lithium only adds mass to the exhaust without adding further energy. This makes the calculation a more conservative estimate. Using the parameter assumptions and reactions in Table 1 to calculate the reaction rate and energy of the products, the total energy and engineering gain is estimated for the pulsed engine operation.

$$E_{fus} = E_{He^3} + E_{He^4} + E_T + E_p$$

$$G = \eta \frac{E_{fus}}{E_{in}}$$

where η is the efficiency of energy transfer from the driver to the load, assumed to be 0.5 and the input energy is calculated as the sum of the magnetic and heating energy added to the plasma to achieve ignition at state 2.

$$\frac{E_{in}}{\eta} = E_{mag,2} + U_2 = \frac{B_2^2}{2\mu_0} V_2 + m c_v T_2.$$

By setting the energy at state 3 equal to the energy of the fusion products plus the energy added to the plasma by heating it to ignition, T_3, the temperature after the

Table 1
Molecular reactions and parameter assumptions.

Pulse frequency	10 Hz
Driver energy density	10 kJ/kg
Compression ratio	10
Initial DT fuel mass	100 mg
Ignition temperature	20 keV

plasma expands in process [2–3] can be calculated:

$$U_3 = (m_l c_{vl} + mc_v)T_3 = E_{fus} + mc_v T_2$$

$$T_3 = \frac{E_{fus} + mc_v T_2}{m_l c_{vl} + mc_v}$$

Thrust and I_{sp} as a function of fractional liner mass $\left(\frac{\text{mass of lithium}}{\text{mass of D–T}}\right)$ were calculated and plotted with Table 1 values in Figs. 5 and 6. The optimum liner mass ratio of 200 (20 g Li^6/0.1 g DT), was chosen to yield a recommended design point of 38 kN thrust and $I_{sp} \sim 19{,}436$ s/pulse.

$$D + T \rightarrow He^4(3.5\,MeV) + n(14.1\,MeV)$$

$$D + D \underset{50\%}{\rightarrow} T(1.01\,MeV) + p(3.02\,MeV)$$

$$D + D \underset{50\%}{\rightarrow} He^3(0.82\,MeV) + n(2.45\,MeV)$$

$$D + He^3 \rightarrow He^4(3.6\,MeV) + p(14.7\,MeV)$$

$$T + T \rightarrow He^4 + 2n + 11.3\,MeV$$

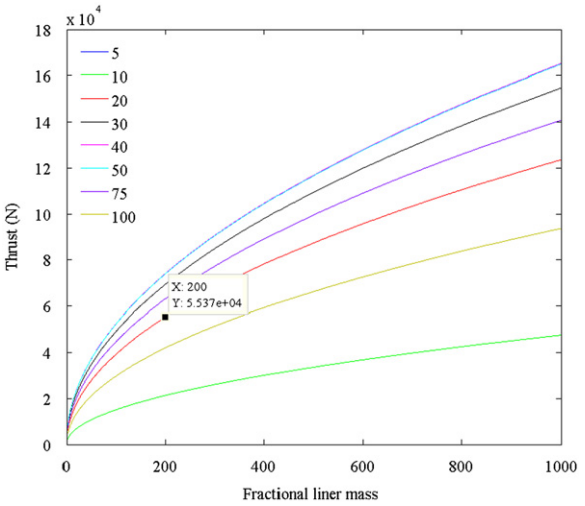

Fig. 5. Thrust as a function of Li Liner Mass Ratio. (For interpretation of the references to colour in this figure legend, the reader is referred to the web version of this article.)

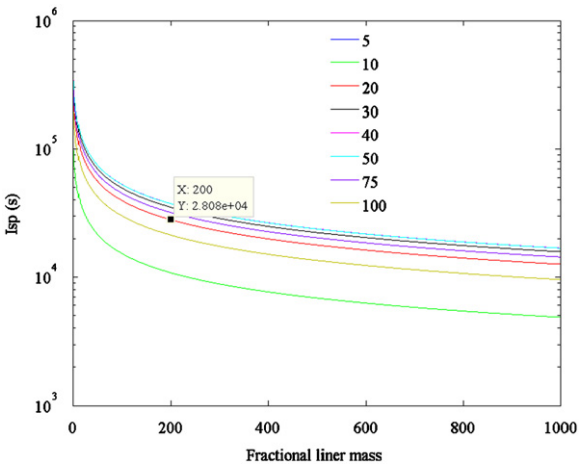

Fig. 6. I_{sp} as a function of Li Liner Mass Ratio. (For interpretation of the references to colour in this figure legend, the reader is referred to the web version of this article.)

3. Results

3.1. Main propulsion concept

After the energy is released during nuclear fusion, a magnetic nozzle converts the released energy into a useful vehicle impulse. The magnetic nozzle is envisioned to be composed of 8 current-carrying rings in a parabolic nozzle shape. Each of the 8 ring assemblies that comprise the nozzle is actually composed of two separate conducting rings as shown in Fig. 7

These rings are positioned to form a parabolic nozzle focused at the point of fusion. As a result, an electrical current passes around each ring and results in a magnetic field as illustrated in Fig. 8, which depicts the entire nozzle in cross-section.

After each fusion event, the plasma is hot and its shell is rapidly expanding. The plasma then begins to compress the magnetic flux into a smaller annular region between the plasma and the rings. As the magnetic flux is compressed, the field strength ($\underline{B}$) increases, as does the magnetic pressure (B^2/μ_0), where μ_0 is the permeability of free space. This acts on the expanding plasma shell, preventing the plasma from contacting/annihilating the rings. An equal and opposite force, much of it is axially upwards along the main axis of the nozzle and the vehicle, transfers the kinetic energy of the plasma pulse to propel the vehicle.

In each of the 8 ring assemblies there is a central superconducting coil that generates the initial seed magnetic field. Before fusion takes place, a magnetic field fills the volume of the nozzle. This coil is a high-temperature superconducting mesh immersed in liquid nitrogen (LN_2) coolant. A yttrium-based superconductor ($YBa_2Cu_3O_7$) is proposed that has a transition temperature of 92 K, which can be maintained by LN_2 at 77 K. The second conducting ring, the "thrust coil," supports the electrical current that is induced during plasma expansion. A metal composite of molybdenum in a matrix of titanium diboride with a very low resistivity would offer good electrical conduction and strength properties at high temperature.

Fluorine–Lithium–Beryllium (FLiBe) is proposed as the main thermal coolant and would flow through channels inside the ring assemblies, as well as through all the Carbon–Carbon (C–C) structures supporting the coils and comprising the nozzle and thrust struts. This fluid is suggested for the dual purpose of heat removal and capturing gamma rays and neutrons. Eight ring assemblies, spaced at equal radial angles from the focal point of fusion, are supported within the C–C parabolic nozzle. The shape and configuration of a ring assembly, shown in cross-section in Fig. 9, would be angled towards the focus of the fusion pulses to allow the FLiBe to

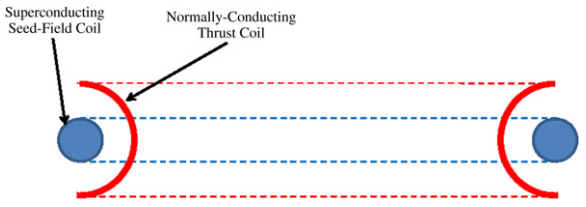

Fig. 7. Cross-section of coils in each ring assembly.

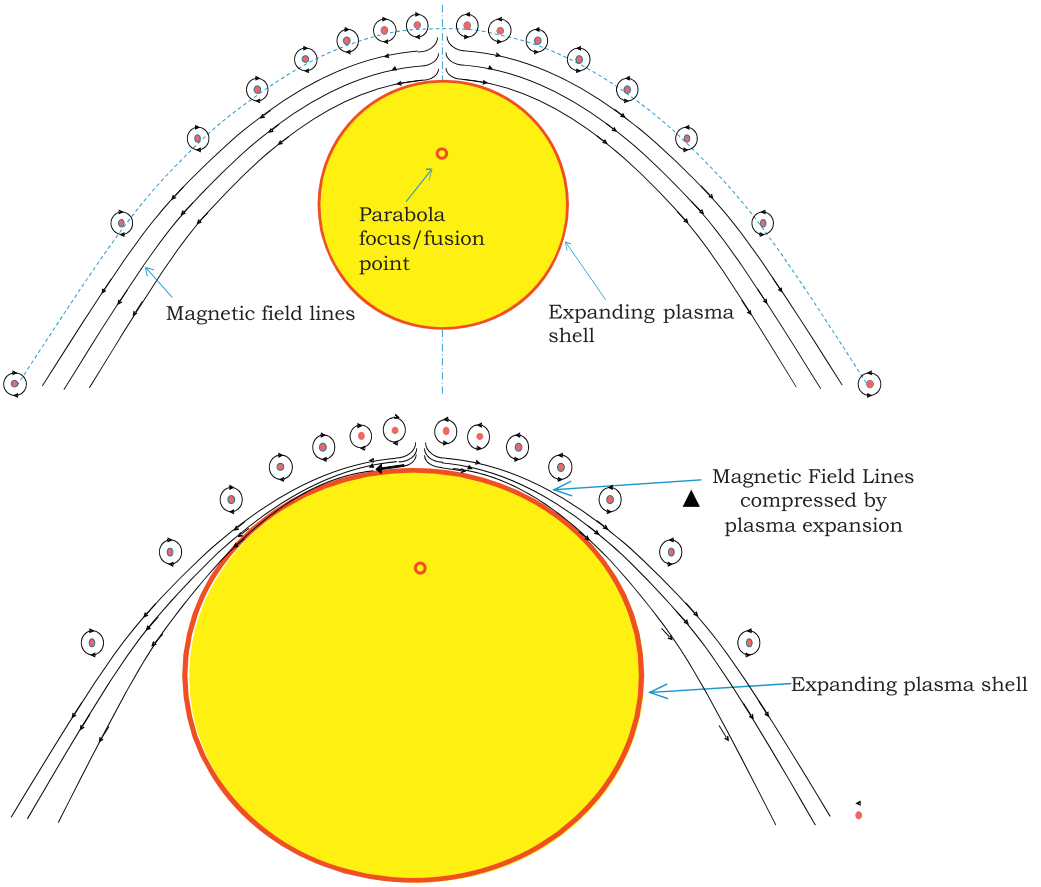

Fig. 8. Magnetic nozzle in cross-section and expanding plasma.

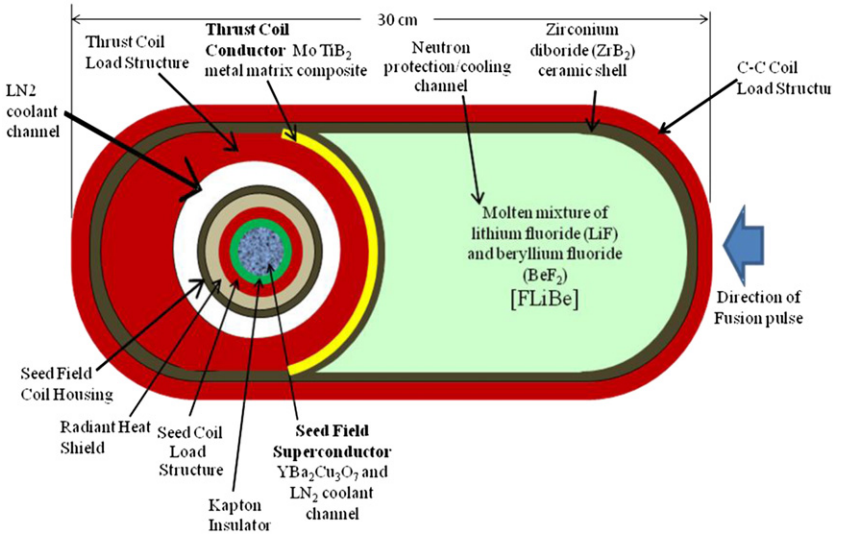

Fig. 9. Cross-section of the structure and shielding around an actively-cooled ring assembly. Dimensions and aspect ratio to be determined after detailed structural analysis.

protect the magnetic conductor coils from neutrons. This radiation protection would be in addition to the Li^6 "liner" which is expected to absorb high energy neutrons and will slow down many more.

Given that the rings are arranged in this shape, the plasma radiating outwards from the focus of the parabolic nozzle will be directed out of the nozzle, parallel to the axis—no matter where it strikes. After the plasma exits,

the magnetic field returns to its original configuration. During this entire process, of plasma expansion and expulsion, the magnetic field acts in the manner of a spring. The magnetic fields are first compressed, and then they expand back to the original configuration—with useful thrust being applied to the vehicle via the thrust coils embedded in the structural C–C nozzle. There are additional structural, cooling, radiation and neutron shielding components incorporated in the design of the magnetic nozzle along with the ring assemblies.

For modeling purposes, the plasma expansion shell is divided into 8 discrete segments. Each is positioned at equal spherical angles from the fusion point, which is by design at the focus of the parabolic nozzle. Fig. 10 shows the actual plasma ejection trajectories modeled.

In summary, the expanding plasma has a total mass of 0.02 kg, and its initial kinetic energy is assumed to be 1 GJ (1×10^9 J). Useful thrust to the vehicle per pulse = 3812 N s and at 10 Hz (10 pulses/s) I_{sp} = 19,436 s. This was used to provide the loads for structural analysis of the magnetic nozzle and ring assemblies shown in Table 2.

3.2. Z-Pinch energy regeneration/discharge system

A large amount of energy must be applied to the DT fuel bolus over a period of just around 100 ns to create the conditions necessary for fusion. To do this, capacitor banks with very low capacitance must be used so that the discharge will be rapid. The banks must be charged to a

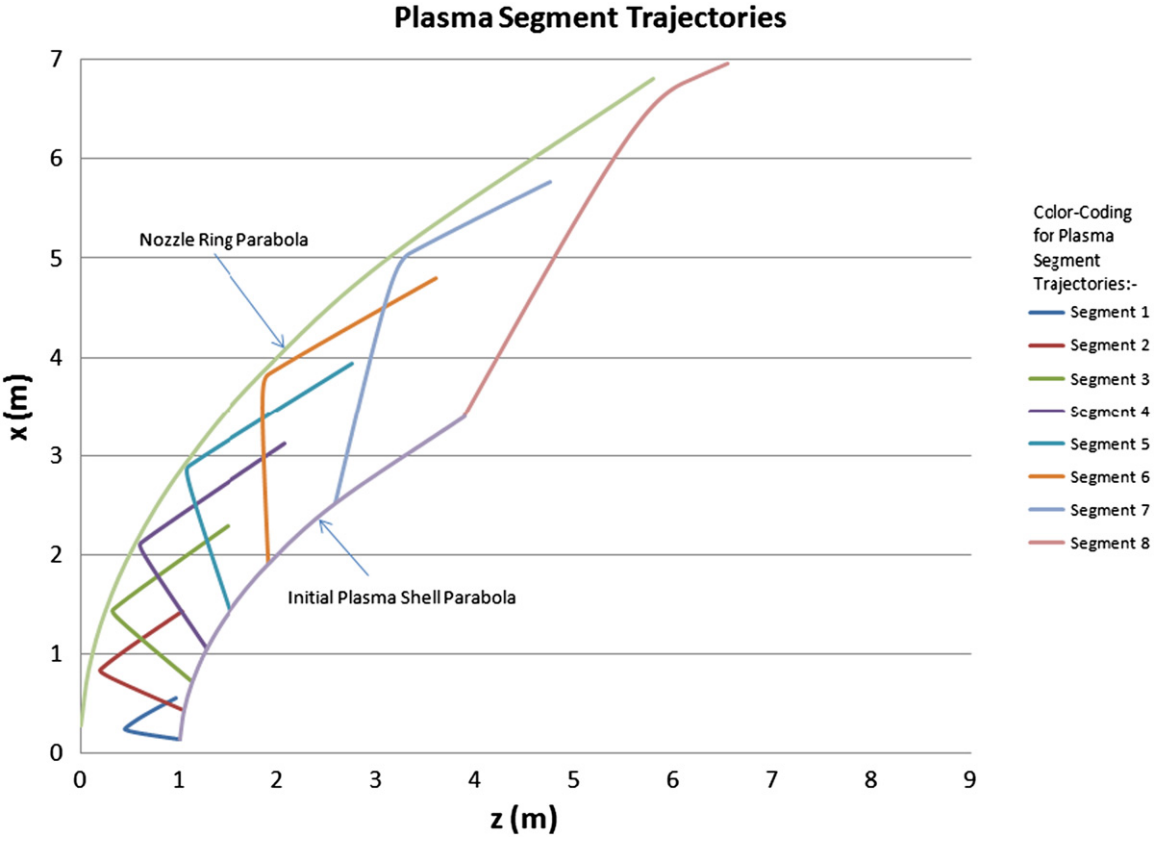

Fig. 10. Plasma trajectories exiting nozzle over 15 μs.

Table 2
Plasma results.

Ring no.	Inductance (T m^2/A)	Initial (seed coil) current (A)	Max. (thrust coil) current (N)	Max. axial force acting on the ring (N)	Max. radial linear pressure acting on the ring (N/m)
1	3.85E−07	2.52E+07	6.58E+07	8.39E+07	2.74E+06
2	2.35E−06	4.13E+06	1.32E+07	5.49E+08	2.20E+07
3	4.99E−06	1.94E+06	6.57E+06	1.38E+09	5.57E+07
4	8.29E−06	1.17E+06	4.39E+06	1.93E+09	7.78E+07
5	1.24E−05	7.79E+05	3.25E+06	1.72E+09	6.95E+07
6	1.79E−05	5.42E+05	2.46E+06	1.03E+09	4.16E+07
7	2.54E−05	3.81E+05	1.83E+06	4.05E+08	1.65E+07
8	3.68E−05	2.63E+05	1.30E+06	1.02E+08	4.20E+06

very high voltage for them to store enough energy. After discharging to create the Z-Pinch, these capacitor banks must be recharged for the next pulse. During each fusion pulse, the current induced in the thrust coils is used to recharge the capacitors. The Z-Pinch regeneration/discharge subsystem consists of circuitry (capacitors, cables, switches, etc.) required to charge and discharge the capacitors.

The thermodynamic model used to size the fusion portion of the propulsion system estimates the Z-Pinch gain at 3: the amount of energy released by the fusion reaction is 3 times the amount of energy required for ignition. Assuming each pulse generates 1 GJ, 333 MJ must be discharged into the DT fuel pulse in 100 ns to initiate fusion. The capacitor charge efficiency is assumed to be 80%, so 416×10^{-6} J must be available in the capacitor bank.

Even though the capacitors must discharge over a 100 ns period, they have a longer period to recharge, assuming a 10 Hz pulse frequency for the propulsion system. Capacitors may be charged in parallel and discharged in series, so a circuit may be devised that allows a large bank of capacitors to be charged over several microseconds and discharged much more quickly with very little loss. This circuit is known as a Marx Generator and, for this application, individual capacitors are sized by traditional physics-based methods according to required voltage and capacitance. The plasma switches and diodes are not sufficiently well characterized to size with a mass estimating relation, so they are sized as 12% of the capacitor mass. Eight sections of capacitors are arranged radially in a ring surrounding the axis of the magnetic nozzle.

Diodes prevent ringing between the capacitive and inductive portions of the circuit, while the plasma switches complete the series discharge circuit as for a typical Marx Generator, which is shown as a schematic in Fig. 11.

3.3. Thermal system

The thermal subsystem, devised during the HOPE study is comprised of three separate heat rejection systems, which are described briefly in the following list and in Fig. 12:

- a low-temperature radiator system for the avionics and crew systems;
- a medium-temperature (800 K) radiator for the fission power plant;
- a high-temperature (1250 K) radiator for the propulsion system waste heat;
- a cryo-fluid management system utilizing He and NaK to cool LN_2 and FLiBe that reject heat from the Superconducting Magnetic Energy Storage (SMES) and magnetic nozzle ring assemblies.

3.4. Structural considerations

Due to the size of this vehicle, it will be necessary for it to be assembled in space. The components must be designed for modular assembly and be small enough for launch on a conceivable heavy launch vehicle. A few components, such as the tanks, would be analyzed for launch loads, but nearly all components will be launched in a stowed configuration. This will produce lower vehicle structural loads, because the vehicle would not be required to withstand launch from Earth as an integrated structure. Most of the vehicle structure will consist of an aluminum truss.

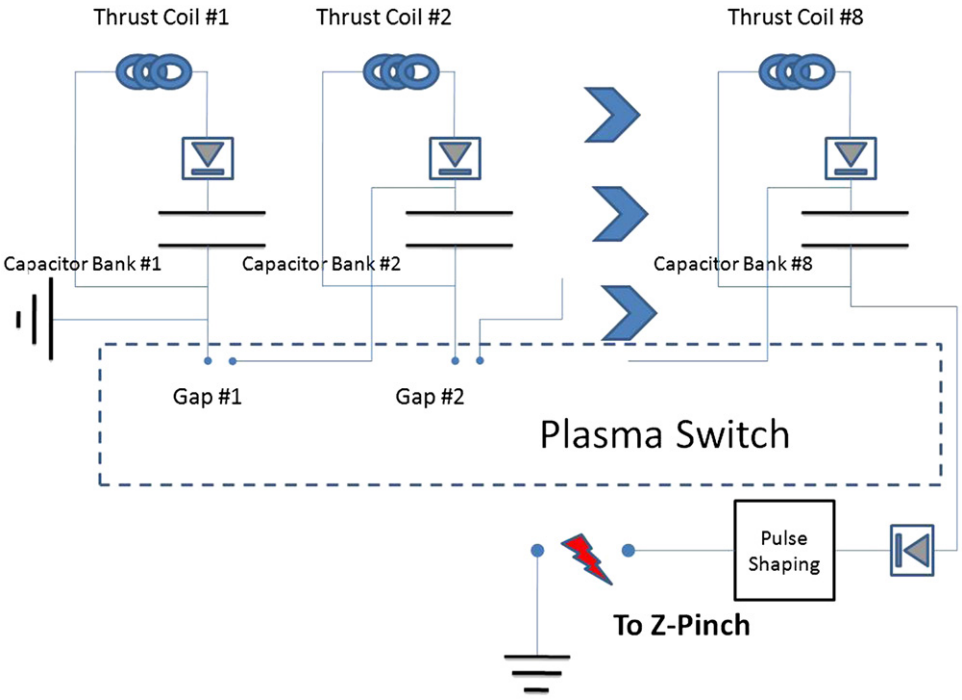

Fig. 11. Basic schematic of the charge/discharge system.

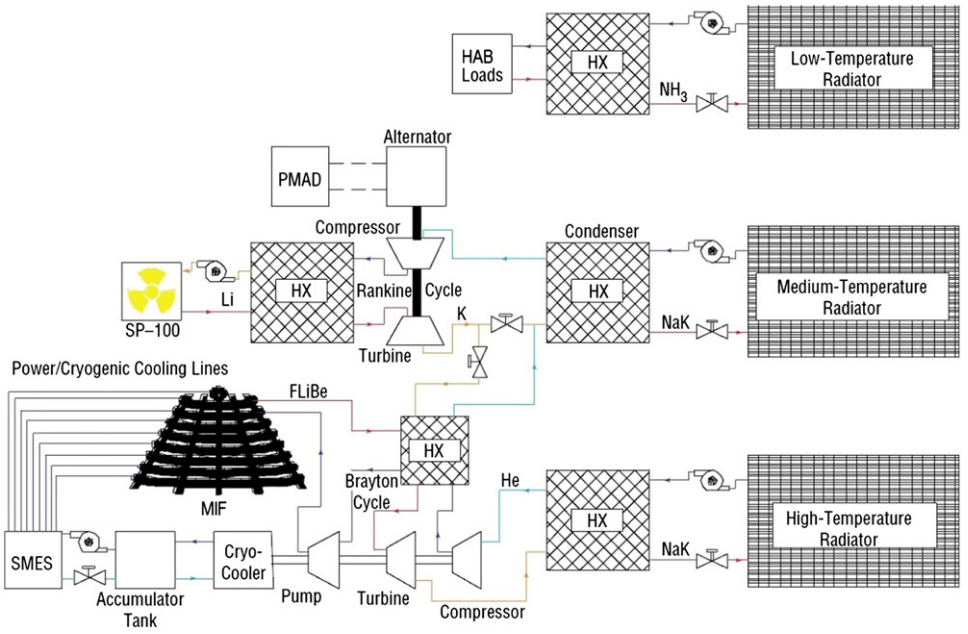

Fig. 12. Vehicle power, thermal rejection schematic.

The 2010 Z-Pinch study configuration is a 125 m long vehicle with the crew compartment and landing vehicles at the front end of a long square truss and the main nuclear propulsion system at the aft end. The engine nozzle and most of the structure to the right of the hashed line shown in Fig. 1 is the HOPE vehicle configuration. The radial capacitor banks are a Z-Pinch design plus a more recent analysis suggests an 8-spline magnetic nozzle with variable spline cross-sections and ring assemblies embedded into 8 structural rings would provide an optimized nozzle design.

The engine nozzle could be made of a Carbon Composite (C/C) material, such as a graphite epoxy composite IM7/8552, to provide stiffness and low mass. The magnetic field generated in the nozzle will protect the nozzle structure from the high-temperature fusion plasma, but, gamma radiation and neutrons will emanate spherically outward from each fusion pulse. Because the capacitor banks must be kept in close proximity to the top of the magnetic nozzle to provide high voltage pulses to the nuclear fuel, they will be particularly susceptible to radiation damage. A radiation shield cap whose composition is detailed in Fig. 13 will extend down from the top of the nozzle, protecting a radial half-angle wide enough to shield the entire vehicle, particularly the capacitor banks.

The dimensions and stress requirements of the magnetic nozzle structure are based on the fusion engine performance, energy and loads/pulse calculated for an approximately 14 m exit diameter nozzle. A simplified Finite Element Model Analysis and Post-processing (FEMAP) model was created to analyze the nozzle structure and optimize its design and mass. Material susceptibility and shielding capability against fast neutrons produced by the fusion process are important in nozzle and vehicle configuration, so a large Margin of Safety (MOS) must be assumed

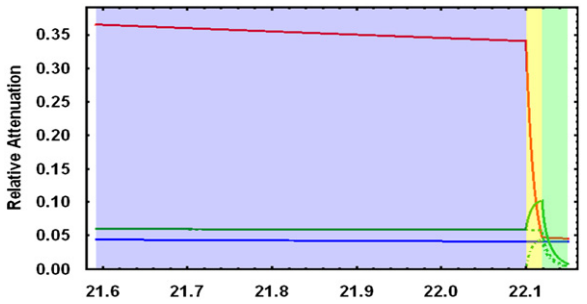

Fig. 13. Radiation shielding thickness: 22 cm, Lithium Hydride (LiH) will capture ~95% of the high energy neutrons. Boron Carbide (B_4C) effectively captures thermal neutrons, but releases gamma rays, and a thin Tungsten layer reduces the gamma rays attenuation: Red = thermal neutrons, Green = gamma rays, Blue = 14.1 MeV neutrons. (For interpretation of the references to color in this figure legend, the reader is referred to the web version of this article.)

for the nozzle structure due to the frequent radiation flux and dynamic stress it must endure, but dynamic frequency and life analysis was not performed. The axial and lateral forces of a fusion pulse are shown in Table 2 and were applied to a segment of the 8 ring assembly; each ring a different diameter and distance from the fusion explosion. The loads are then transmitted through structural splines and struts against the base of the vehicle truss. A fixed boundary that represented a very large mass is placed at the top of the struts, as a conservative approximation. After the model was meshed, a positive static FEA result was obtained with a FEMAP/NASTRAN solver using Titanium and C–C material properties. A simplified thick-walled tubular model of 1/8 of the nozzle, representing thermal fluid channels, was optimized with varying wall thickness rather than cross-sectional dimension, for minimum mass.

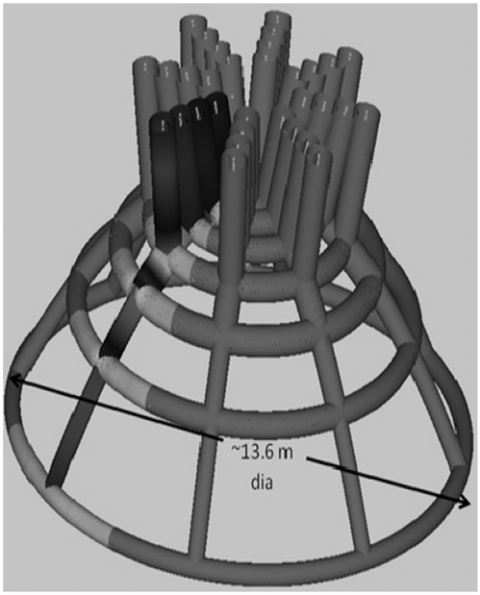

Fig. 14. Revolved FEA model of magnetic nozzle.

The positive FEA result of the sectional model on the left side of the nozzle in Fig. 14 was revolved 360° to obtain the nozzle concept shown.

3.5. Mission analysis for a best estimate vehicle mass

The thrust levels of a Z-Pinch fusion rocket are similar to traditional chemical propulsion systems; however, the mass of the propulsion system results in accelerations in the milli-g range. The outstanding specific impulse of the propulsion system enables high overall system performance. Traditional chemical propulsion systems operate in the 1 g acceleration range, allowing for the assumption of impulsive burns for trajectory analyses because the burn time is relatively short compared to the overall trip time. The Z-Pinch propulsion system's milli-g accelerations places it in the category of "medium thrust" trajectory analysis, so the burns were numerically integrated and patched into a transfer conic trajectory.

Several simplifying assumptions were made for this analysis. No ephemeris data and simple circular orbits at the mean orbital radius were used to represent the departure and arrival planets. While the results are valid for required transfer energies, the epoch of the mission and stay time at the destination were not quantified in this analysis. The arrival conditions for each leg were set at a v infinity of 0 km/s. The planetary orbit component of the trajectories was not assessed and no parking orbit analysis was performed. Escape burns should account for approximately 10% of the propellant load, but they have not been assessed in this analysis.

For a given payload mass of 150 mT, Z-Pinch offers a 50% reduction in the nominal one-way trip time compared to a chemical propulsion mission. The 90-day trajectory has a 1.5 day Earth departure burn. The total burn time is 5 days for a roundtrip Mars mission, equating to 27,500 m/s of ΔV and using 86.3 mT of propellant. The trajectory for a 30-day trip to Mars requires an 8.7 days Earth departure burn. For a roundtrip, this trajectory requires a total burned propellant load of 350.4 mT and has an equivalent ΔV of 93,200 m/s. While these numbers are significantly larger than the 90-day trajectories, this does show the feasibility of a 30-day trip to Mars. Trip time, propellant, and ΔV are compared in Table 3 for a vehicle with a 552 mT burn-out mass, which is in the range of the study's "Best Estimate" mass shown in Table 4.

Table 3
Trip time, propellant and ΔV.

552 mT burn-out mass	Mars 90 days one-way	Mars 30 days one-way
Outbound trip time (days)	90.2	39.5
Return trip time (days)	87.4	33.1
Total burn time (days)	5.0	20.2
Propellant burned (mT)	86.3	350.4
Equivalent DV (km/s)	27.5	93.2

Table 4
Vehicle mass estimate breakdown for 90-day Mars roundtrip.

Subsystem	Mass (kg)
Payload—crew habitat, lander, small transport, radiation protection, and consumables	150,000
Structures—main truss, main propulsion tanks, secondary structure for systems below	31,500
Main propulsion—MIF nozzle, magnetic coils, radiation shielding, capacitors/Marx generator system	115,000
Thermal management—radiators, pumps, tanks, cryo-coolers, thermal fluids	77,000
Power systems—fission reactor, radiation shield, distribution lines	16,500
Avionics and RCS—control boxes, sensors, communication and reaction control system	2300
30% Mass growth allowance	117,700
Main propulsion and RCS propellant—for 90-day Mars roundtrip	87,900
Total mass (best estimate)	597,900

4. Discussion—future work

The technology development required for this propulsion system is achievable on a reasonable timescale given sufficient resources. The first stage of a development program would involve sub-scale experiments to establish the foundational aspects of the system, such as Z-Pinch formation utilizing annular nozzles. Furthermore, the experiments would yield quantitative information enabling more sophisticated configurations for test and evaluation. The ACO study provided a tangible vehicle concept for the application of Z-Pinch fusion propulsion and aided in the successful proposal bid to fund utilization of the DM2 module in a propulsion development program at Redstone Arsenal (RSA).

Several key technologies that warrant development to produce the first fusion propulsion system are listed in Table 5. These are covered in the development plan envisioned for the Z-Pinch Test Facility at RSA, in Huntsville, Alabama.

Table 5
Key Technology Readiness Levels (TRL) estimates.

	TRL level
High temperature Z-Pinch	4
Intense electrical pulse power	4
Magneto-hydrodynamic electricity	5
Thermonuclear equations of state	3
Dynamic plasma radiation shielding	3
Advanced structures	2
Reaction containment	2

DM2 stands for Decade Module 2, a ~500 kJ pulsed power facility. The DM2 was the last prototype serving as a test bed for the design and construction of the much larger Decade Machine. DM2 is one of the latest inductive energy storage, pulse power machines and is an excellent research platform for a university pulsed power or plasma physics research branch. Despite over 10 years of use, the unit is in good working order and has had a reliable operating history. UAHuntsville has arranged for the transfer of government equipment to a UAHuntsville-managed secure facility located on the Redstone arsenal in Huntsville, Alabama.

Experiments carried out on wire array Z-Pinch machines use multiple diagnostic methods to observe the behavior of the implosion process from initiation to stagnation. Experiments carried out with the DM2 Z-Pinch module will also accommodate the same diagnostic methods. Eventually, the demonstrated proof of break-even energy production must be established to justify the construction of a fusion propulsion engine. A break-even facility is one that puts out as much or more energy as the input.

5. Conclusions

Fusion-based nuclear propulsion has the potential to enable fast interplanetary transportation. The large size of an interplanetary vehicle dictates that it will be assembled in space. Due to the great distances between the planets of our solar system and the harmful radiation environment of interplanetary space, high specific impulse (I_{sp}) propulsion vehicles with high payload mass fractions have a practical advantage of providing fast transit through a hazardous environment for human space flight missions.

Analysis of the Z-Pinch propulsion system concludes that a 40-fold increase of I_{sp} over chemical propulsion is predicted. An I_{sp} of 19,436 s and useful thrust of 38 kN for 150 mT payload, a nearly doubling of the predicted payload mass fraction, warrants further development of enabling technologies.

The vehicle can be designed for multiple interplanetary missions and conceivably may be suited for an automated one-way interstellar voyage.

Acknowledgments

The Advanced Concepts Office at Marshall Space Flight Center (MSFC) thanks William Emrich, also at MSFC, for help in radiation shielding and Dr. Bill Seidler, senior technical fellow at The Boeing Co., who was actively involved in the DECADE program and is facilitating the communication between UAHuntsville and providing invaluable mentoring in DM2 utilization.

References

[1] I. Lindemuth, R. Siemon, The fundamental parameter space of controlled thermonuclear fusion, Am. J. Phys. 77 (5) (2009) 407–416.
[2] A.L. Velikovich, C.L. Ruiz, et al., Z-Pinch plasma neutron sources, Phys. Plasmas 14 (2) (2007) 022701, doi:10.1063/1.2435322.
[3] R.B. Adams, G. Statham, Y.C.F. Thio, et al., Conceptual Design of In-Space Vehicles for Human Exploration of the Outer Planets, NASA/TP-2003-212691, 2003.
[4] T. Polsgrove, R.B. Adams, G. Statham, J.H. Miernik, J. Cassibry, J. Santarius, et al., Z-Pinch Pulsed Plasma Propulsion Technology Development, NASA Report M11-0145, 2010.
[5] C.E. Olson, Development path for Z-Pinch IFE, Fusion Sci. Technol. 47 (2005) 633–640.
[6] U. Shumlak, R.C. Lilly, C.S. Adams, R.P. Golingo, S.L. Jackson, S.D. Knecht, et al., Advanced space propulsion based on the flow-stabilized Z-Pinch Fusion. In: Proceedings of the 42nd AIAA/ASME/SAE/ASEE Joint Propulsion Conference ,2006, pp. 1–14.
[7] J.F. Santarius, Magnetized-Target Fusion for Space Propulsion, NASA Project NAG8-1719, 2003.